SEPTIEME COLLOQUE SUR LE TRAITEMENT DU SIGNAL ET SES APPLICATIONS

NICE du 28 MAI au 2 JUIN 1979

A NEW DIGITAL ADAPTIVE BEAMFORMING SYSTEM FOR MICROWAVE RADAR ARRAYS

Lloyd J. Griffiths and Charles W. Jim

Department of Electrical Engineering, University of Colorado, Boulder, Colorado 80309 U.S.A.

RESUME

Cette étude décrit un system hybride, analogue/digital et spatialement adaptif pour traitement d'arrangements d'antennes, leguel peut être utilisé pour arrangement en haute fréquence et large bande. La structure proposeé est unique en ce sens qu'elle emploie de simples éléments de filtrage analogue dans le générateur de rayonnement et que ces filtres sont adaptés moyennant un computer digital utilisé en mode "off line" et une version modifiée de l'algorithme des moindres carrés. Par conséquent, les signaux de grande cadence reçus des arrangements d'antennes traversent des éléments analogues et une rapide conversion analogue/digital n'est pas requise at ce rythme.

Cependant, le générateur de rayonnement conserve la fléxibilité d'un arrangement entièrement digitalisé. En conséquence, un filtrage spatial/temporel est acquis au sein de la largeur de bande de l'arrangement d'antennes.

Ceci contraste avec les précédentes approches au générateur de rayonnement en micro-ondes, lesquelles employaient des éléments analogues à déplacement de phase et sont restraintes au filtrage spatial en bande étroite.

Le system adaptif de génération de rayonnement proposé est un éffaceur multidimentionnel de bruit dans lequel seulement les signaux de bruit sont dérivés en attaquant un simple préprocesseur spatial par les sorties des éléments de l'arrangement. Ces signaux de pur bruit sont alors filtrés à travers des lignes à retard dont les coéfficients sont restraints aux trois valeurs possibles: -1, 0, +1.

Au sein de cette étude, nous présentons une description analytique et simplifiée du processeur ainsi que l'algorithme adaptif modifié. Des expériences de simulation sont aussi présentées qui illustrent les performances du processeur.

SUMMARY

This paper describes a hybrid, analog/digital spatially-adaptive antenna array processing system which can be used in high-frequency, widebandwidth arrays. The proposed structure is unique in that simple analog filtering elements are employed in the beamformer and these filters are adapted using an off-line digital computer and a modified least-mean-square algorithm. Thus, the high-rate received array signals flow through analog elements and high-speed A/D conversion at these rates is not required.

The beamforming system does, however, maintain the flexibility provided by a fully digital array. As a result, combined spatial/temporal filtering within the array bandwidth is achieved. This is in contrast to previous approaches to adaptive beamforming at microwave frequencies which have employed analog phase-shifting elements and are restricted to narrowband spatial filtering.

The proposed adaptive beamforming system is a multidimensional noise canceller in which noise-only signals are derived by passing the array element outputs through a simple spatial preprocessor. These noise-only signals are then filtered using tapped-delay-lines having tap weights which are restricted to three possible values: -1, 0, +1.

In this paper, we present a simplified analytical description of the processor and the modified adaptive algorithm. Simulation experiments illustrating the performance of the processor are also presented.

A NEW DIGITAL ADAPTIVE BEAMFORMING SYSTEM FOR MICROWAVE RADAR ARRAYS

I INTRODUCTION*

Adaptive receive-array beamforming systems which steer nulls in the direction of strong interfering signals were first proposed by Mermoz [1] in 1963 for use in sonar systems. Since that time, adaptive receive-array processing has been used in a variety of acoustical and radio wave applications [2,3,4]. These systems may be classified as being one of two basic types: 1) digital adaptive beamformers which employ analog-to-digital (A/D) conversion directly at the element outputs (or after individual receivers connected to each element) and 2) analog adaptive beamformers which utilize variable gain/phase networks at the output of each element.

The digital approach offers the advantage of flexibility in processing. A wide variety of algorithms have been suggested based on either time-domain gradient procedured [5], or on matrix inversion methods [6]. Digital processing also allows the possibility of frequency-domain beamforming, in which a Fourier Transform of each element output is taken prior to beam formation. In this case, different adapted beams are formed for each frequency bin using a single complex weight for each frequency. Time-domain methods accomplish similar processing using a tapped-delay-line or finite impulse response (FIR) filter at each element output. The beamformed output, however, consists of a single, frequency-dependent adaptive beam. Because of the frequency dependence of these systems, digital beamforming is often termed broadband processing. Typically, digital systems are employed in those applications in which the array bandwidth is a significant fraction (10% or greater) of the received center frequency. Examples have been presented in sonar and seismic applications as well as in radio frequency systems which utilize down-conversion receivers at each element. Systems of this latter type must include provisions for gain and phase matching of these receivers to preserve the integrity of the desired signal.

The upper frequency limit of digital adaptive beamformers is determined by the maximum available speed of A/D, digital multipliers, adders, and shift registers. Even with high-speed devices, this limitation imposes a severe limit on bandwidth. As an example, consider a 32-element array which has 10 coefficient FIR filters at each element. (Equivalently, 10 frequency resolution cells.) This system requires 320 multiplies and adds per input sample to compute a beam with fixed, non-adaptive weights in the filters. If, in addition, an adaptive algorithm is used (e.g., Widrow's LMS algorithm) to update the weights, an additional 320 operations per sample are needed. Thus, even at digital hardware speeds as high as 600 kHz, the effective sampling rate is reduced to less than 1 kHz due to the computational load of 640 operations per sample. Although parallel processing can increase this rate significantly, added digital complexity is needed, which may impose unacceptably large costs on the overall system. Because of these factors, digital systems for adaptive array processing have been restricted to operating bandwidths of less than a few tens of kHz.

Adaptive arrays which operate at several hundred MHz have been constructed, however, using analog methods. These systems employ analog feedback loops containing integrators and/or correlators to perform the weight adaptation operations. Typically, two weighting factors are used at each element, one each for phase and gain control. Again, this control is achieved using analog circuitry. Because analog elements which perform the full range of processing provided in digital arrays have not yet been developed, analog adaptive arrays have been restricted to narrowband processing, i.e., systems with a bandwidth which is a small fraction of the carrier frequency. The bandwidth restriction usually arises due to the limitations imposed by the requirement for a constant 90° phase shift over the frequency range of the received signals. At larger bandwidths, gain/phase processing may provide insufficient interference rejection -- particularly if the interfering signal spectrum is not constant over the received bandwidth. In these cases, tapped-delay-line structures have been shown to provide significantly improved performance [7] when compared with gain/phase processing. Analog adaptive tapped-delay-lines have not been developed, however, due to the inherent complexity of such devices.

This paper suggests a new approach to digital adaptive processing in arrays which is based on the use of a hybrid analog/digital beamforming system. The proposed system uses an analog beamforming network consisting of tapped-delay-lines in which the taps are constrained to have values of +1, -1 or zero. Thus, the taps are implemented with simple switching elements and are easily obtained with analog elements. Digital processing is used to select the tap values and takes place using an off-line digital computer. The computer receives digitized inputs from the array element signals and from the analog beamformed output signal, as shown in Fig. 1. A single variable analog gain element, shown as γ in Fig. 1, is also controlled by the off-line processor.

The A/D units shown must be capable of sampling at the center frequency of the array, which may be as high as several hundred MHz. Note, however, that because the received signals are processed using analog components, there is no requirement to operate the A/Ds at a sampling rate greater than the Nyquist rate for these signals. Instead, samples are taken at a rate sufficiently high to allow the adaptive processor to track time variations in the input signals. For most applications of interest, these variations are likely to occur at rates lower than a few kHz. The requirements on the A/D elements are then 1) an aperture time which is short compared with the period of the center frequency of the array, and 2) a sampling rate which can be varied down to rates as low as a few kHz. Devices which meet these requirements have recently been reported by TRW Systems, Inc. [8]. They are based on the use of transfer electron devices and operate at rates as high as 5 gigasamples per second. The aperture time remains at about 150 picoseconds for sample rates between DC and 5 Gs/sec. At present, the number of output bits per sample from these elements is limited to low-order bits only - i.e., to 2 or 3 bits resolution. It is shown in the sections following, however, that this resolution is sufficient to provide a large amount of interference rejection in high-frequency adaptive arrays which use the hybrid processor illustrated in Fig. 1.

* This work was supported by the Office of Naval Research, Washington, D.C. under Contract No. N 00014-77-C-0592.

II FORMULATION OF HYBRID ADAPTIVE ARRAY PROCESSOR

The signals present in the processor shown in Fig. 1 are conveniently described using vector notation. Specifically, if $x_m(t)$ is used to denote the signal observed at the output of the m^{th} array element at time t, and $\underline{X}(t)$ is the M dimensional vector of these signals, then

$$\underline{X}^T(t) = [x_1(t); x_2(t); \ldots, x_M(t)] \quad (1)$$

where T denotes transpose. The upper path of the array processor forms a conventionally-weighted beam $y_c(t)$ using weights c_i. Thus,

$$y_c(t) = \underline{X}^T(t)\ \underline{W}_c \quad (2)$$

where $\underline{W}_c^T = (c_1; c_2; \ldots, c_M)$.

The processing configuration shown in Fig. 1 is termed a generalized sidelobe canceller due to the fact that the purpose of the lower, adaptive path is to subtract out interference terms present in the conventional beam $y_c(t)$. This is accomplished through the use of a prefilter $\underline{\underline{W}}_s$ which blocks the desired array signal from the lower path. We assume that the array has been presteered (either mechanically or electronically) in the direction of interest such that the array output signals $x_m(t)$ may be expressed as

$$x_m(t) = s(t) + n_m(t) \quad (3)$$

Thus, the desired signal s(t) appears in phase at each output. If $\underline{\underline{W}}_s$ is viewed as a fixed matrix operation with output vector $\underline{X}'(t)$,

$$\underline{X}'(t) = \underline{\underline{W}}_s \underline{X}(t) \quad (4)$$

then $\underline{X}'(t)$ contains no s(t) terms. This can be accomplished in a number of ways - for example, by subtracting adjacent element outputs - and results in a vector $\underline{X}'(t)$ which has dimension one less than the number of array elements.

An adapted beam output $y_a(t)$ is formed by passing the vector $\underline{X}'(t)$ through a set of tapped-delay-lines having tap values of +1, -1, or 0. Assuming an interval delay of τ seconds (typically one-half wavelength at the array center frequency), the formulation for $y_a(t)$ is given by

$$y_a(t) = \gamma_k \sum_{\ell=0}^{L} \hat{\underline{W}}_\ell^T(k)\underline{X}'(t-\ell\tau) \quad (5)$$

where $\hat{\underline{W}}_\ell^T(k) = [1; -1; 0; 0 \ldots, -1]$ (typically) (6)

is the vector of tapped-delay-line weights after the ℓ^{th} delay element and γ_k is an adaptively controlled gain factor. The elements of each $\hat{\underline{W}}_\ell(k)$ are also adaptively updated using a simple gradient approach which is designed to minimize the average power contained in $y_o(t)$. Since $y_a(t)$ contains only noise and interference-related terms ($\underline{\underline{W}}_s$ blocks the desired signal from the lower path), minimizing $\langle y_o^2(t)\rangle$ results in a minimization of output noise and interference.

If the tapped-delay-line elements in Fig. 1 are not constrained to values of +1, -1, and 0, the weight values can be adapted using the well-known LMS algorithm developed by Widrow [2]. It can be shown that the hybrid digital processor will converge to the optimal solution using the following implementation of that algorithm which requires two A/D converters. In order to update the weight located on the m^{th} delay line after ℓ delays $w_{m,\ell}(k)$, the two converters are used to obtain time-synchronous samples of the output $y_o(t)$ and the signal present at the weight of interest, $x'_m(t-\ell\tau)$. Assuming that these samples are taken at time $t = t_k$ and using the symbol $\sim$ to denote the quantized outputs of the A/D converters, the Widrow LMS algorithm for an individual weight is given by:

$$w_{m,\ell}(k+1) = w_{m,\ell}(k) + \frac{\alpha}{\sigma_m^2(k)} \tilde{y}_o(t_k)\tilde{x}'_m(t_k-\ell\tau) \quad (7)$$

In this expression, $0 < \alpha < 1$ is a step size parameter which controls the convergence properties of the algorithm and $\sigma_m^2(k)$ is an estimate of the power content in the m^{th} channel. Typically, $\sigma_m^2(k)$ is updated using a single-pole filter of the form

$$\sigma_m^2(k) = (1-\alpha)\sigma_m^2(k-1) + \alpha[\tilde{x}'(t_k-\ell\tau)]^2 . \quad (8)$$

In systems with AGC, this term may be replaced by an appropriate constant.

The algorithms shown in (7) and (8) are easily implemented in a small, general-purpose digital processor and will result in a beamformer which converges smoothly to the optimal solution as the A/D converter cycles through the totality of signals in the delay lines. (Note that each delay line sample must be accompanied by a time-synchronous output sample taken with the second A/D converter.) Unfortunately, however, these algorithms are not appropriate for the case of the constrained delay-line weights of interest in this paper. Quantizing the weights to values of +1, -1, or 0 after applying the LMS algorithm in (7) is also invalid.

To understand why the LMS algorithm fails, consider the case of a two-weight system illustrated in Figure 2. This illustration shows error surface contours for a hypothetical problem having optimal unquantized weights w_1^* and w_2^*. If the weights are constrained to have values of +γ, -γ, or 0 (as is the case in Fig. 1 due to the presence of the multiplying constant γ), then the quantized weights must lie along one of the $3^N - 1 = 8$ "spokes" given by the 4 major axis and the 4 diagonals. The optimal quantized coefficients are shown as $\hat{w}_1$ and $\hat{w}_2$.

If one uses the LMS algorithm in (7) with appropriate quantization, it is possible to reach a "trapped-state" situation in which the weight vector is restricted to lie on a suboptimal spoke. Figure 3 illustrates this trapping. With an initial vector of (0,0), the LMS gradient measured is shown by dotted arrows. At each iteration, the weights are quantized to the nearest spoke. The numbers 1,2,3 show the resulting sequence. The final adapted vector will lie near point 3 and a jump to the superior diagonal spoke (which contains the optimal quantized weights) will never occur if the distance to the spoke exceeds the gradient step size. Increasing the step size α does not provide a tractable solution, due to the increased adaptation noise which results, and the possibility of an unstable

algorithm ($\alpha > 1$).

In this paper, we propose an "accumulated-gradient" LMS algorithm which overcomes this trapping. Briefly, the method consists of retaining a "virtual" weight vector in the digital processor which does not have its elements quantized to $+\gamma$, $-\gamma$, and 0. This virtual weight vector is updated using the gradient measured by the quantized weight vector and thus tracks according to the accumulated observed gradients. Quantization then takes place using the virtual weight vector. When this quantization results in a jump to the new spoke, the virtual vector is set equal to the quantized vector and begins accumulating gradients anew.

It has been shown that this procedure results in a vector which brackets the optimal quantized solution and does not become trapped. Figure 4 illustrates the weight path produced by this procedure for the hypothetical problem. Mathematically, the procedure is described as follows: Let $\underline{W}_\ell(k)$ $\ell = 0,1,\ldots,L$ represent the set of unquantized virtial weight vectors stored in the digital processor and $\underline{\hat{W}}_\ell(k)$ the corresponding set of quantized vectors having elements +1, -1, or 0. (A simple minimum distance rule is used to find the set $\gamma_k\underline{\hat{W}}_\ell(k)$ which lies closest to $\underline{W}_\ell(k)$ and γ_k is used to set the gain term shown in Fig. 1.) A new virtual weight vector $\underline{W}_\ell(k+1)$ is obtained using the LMS algorithm in (7) and cycling through the totality of $(M-1)\times(L+1)$ weights. Note that this procedure uses the previous virtual vector component $w_{m,\ell}(k)$ on the right-hand side of (7) and not the quantized value. Once all elements of $\underline{W}_\ell(k+1)$, $\ell = 0,1,\ldots,L$ have been obtained, the quantizing rule is used to find $\gamma_{k+1}\ \underline{\hat{W}}_\ell(k+1)$. If this rule results in a switch to a new spoke, the $\underline{W}_\ell(k+1)$ are set equal to the $\underline{\hat{W}}_\ell(k+1)$ and the procedure continues. If a spoke change is not produced (i.e., only γ_k changes), then the $W_\ell(k+1)$ keep their new virtual values. It should be noted that resetting the $\underline{W}_\ell(k+1)$ when a spoke change occurs is mandatory to ensure stability of the algorithm. Specific examples illustrating its performance on synthesized data sets are given in the next section. Results obtained using field-recorded HF radio data have also been obtained and will be presented at the symposium.

III RESULTS OBTAINED USING HYBRID ADAPTIVE ARRAY PROCESSOR

Simulation experiments have been conducted to evaluate the performance of the hybrid adaptive array processor described above. The array was modeled as linear with eight equally-spaced elements. The conventional beamformer weights c_i were Dolph-Tchebychev designed to provide 25 dB sidelobes. The A/D converters were assumed to have 2-bit accuracy with 3 output levels centered on zero. A simple adjacent element difference structure providing seven outputs was used for the $\underline{\underline{W}}_s$ matrix. The digital processor was modeled as having 16-bit accuracy -- corresponding to typical commercially available microprocessors. The desired input was modelled as consisting of a sinusoid incident at 0^o (broadside) and having a Doppler frequency of +25 Hz. The interference was incident at an azimuth of 54^o and consisted of a 100 percent AM modulated sinusoid centered at -15 Hz Doppler. Uncorrelated background noise was also presumed to be present at each array element.

Figure 5 shows the Doppler spectrum observed at the conventional array output for this test. The three Hz AM sidebands are readily apparent in this display. Two curves are shown, corresponding to the peak and RMS levels observed in each Doppler bin over the 1 kHz operating range of the system.

The spectrum observed at the output of a fully-digital high-resolution (60-bit) adaptive array is shown in Fig. 6. Tapped-delay-lines with four adaptive weights were used at each element. As expected, the interference has been effectively removed. The corresponding beam patterns for the adaptive processor are presented in Fig. 7. Note that the processor has a frequency-dependent beam response within the system operating bandwidth. The two curves shown in Fig. 5 correspond to the minimum value of the pattern over this bandwidth and the RMS pattern with those minima removed. A deep null, which is approximately 38 dB below the conventional beamformer response, was produced in the direction of the interfering signal.

The Doppler spectrum and beam pattern observed at the output of the low-order hybrid adaptive system are shown in Figs. 8 and 9, respectively. Again, four-weight delay-lines were used at each element, but the weights in this case were restricted to values of +1 , 0, or -1. The interference is equally well removed from the Doppler spectrum and the pattern null is approximately 30 dB below the conventional response.

IV SUMMARY

This paper has described a hybrid analog/digital beamforming structure designed for use with radio frequency receiving arrays operating at frequencies of several hundred MHz. The components required for the structure are readily available and do not involve the use of special purpose devices. The system will operate directly at the received frequency range and individual element receivers and IF filtering are not required. Preliminary experimental results indicate that good interference rejection is obtained using 2-bit A/D converters and tapped-delay-line weights restricted to values of +1, -1, and 0.

It is somewhat remarkable that deep spatial nulls can be obtained with quantization as crude as described above. One geometric explanation for this performance can be given in terms of the dimensionality of the system. As mentioned in the previous section, an N weight system has a quantized weight vector which is restricted to lie on one of 3^N-1 spokes. An unquantized weight vector can be placed at any point on the surface of the N sphere. One can measure the density of quantization points using the ratio of the number of spokes to the area A(N) of a unit N-sphere. Because A(N) decreases monotonically to zero for $N > 5$, this ratio increases faster than 3^N for large N. Clearly, for values of N in the range 50-100, little quantization error is incurred.

References

1. H. Mermoz, "Adaptive Filtering and Optimal Utilization of an Antenna," U.S. Bureau of Ships (translation 903 of Ph.D. thesis, Institute Polytechnique, Grenoble, France), October 4, 1965.

References, Continued

2. B. Widrow, et al., "Adaptive Antenna Systems," Proc. IEEE, Vol. 55, No. 12, December 1967.

3. J. Capon, et al., "Multidimensional Maximum-Likelihood Processing of a Large Aperture Seismic Array," Proc. IEEE, Vol. 55, No. 2, February, 1967.

4. L. Griffiths, "Time-Domain Adaptive Beamforming of HF Backscatter Radar Signals," IEEE Trans. Antennas and Prop., Vol. AP-24, No. 5, September, 1976.

5. O.L. Frost, III, "An Algorithm for Linearly Constrained Adaptive Array Processing," Proc. IEEE, Vol. 60, No. 8, August 1972.

6. I.S. Reed, et al., "Rapid Convergence Rate in Adaptive Arrays," IEEE Trans. AES, November 1974.

7. L. Griffiths, "A Comparison of Quadrature and Single-Channel Receiver Processing in Adaptive Beamforming," IEEE Trans. Ant. Prop., Vol. AP-25, No. 2, March 1977.

8. D. Claxton, et al., "TED IC Technique Evaluation and A/D Cell Development," Final Report, Office of Naval Research Contract N 00014-76-C-0793, TRW Systems Inc., Redondo Beach, Calif., 90278.

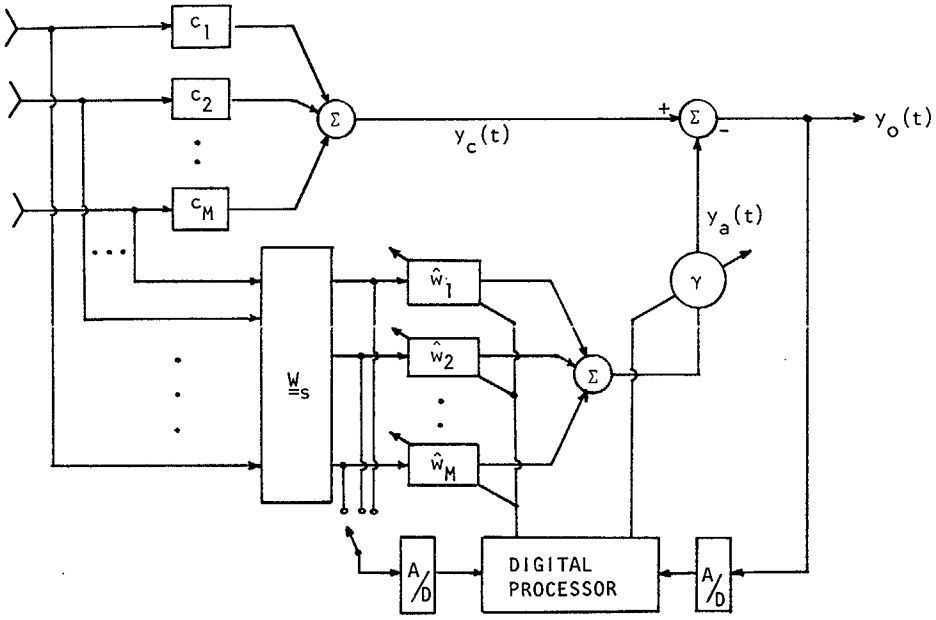

Fig. 1. Hybrid adaptive beamforming configuration.

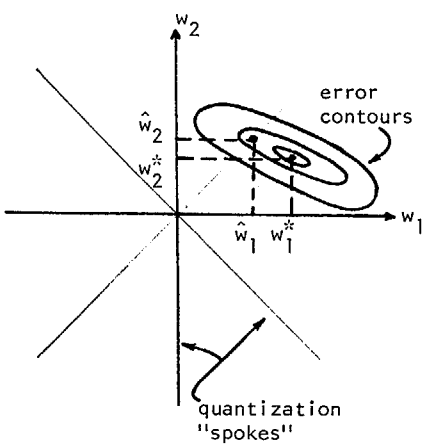

Fig. 2. Two dimensional hypothetical example.

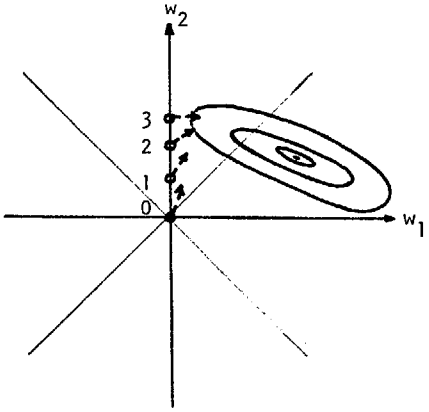

Fig. 3. Weight history using quantized LMS algorithm.

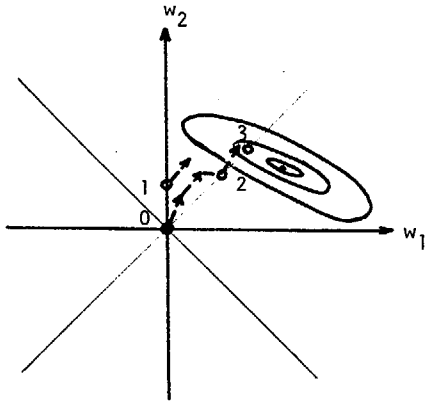

Fig. 4. Weight history using accumulated gradient.

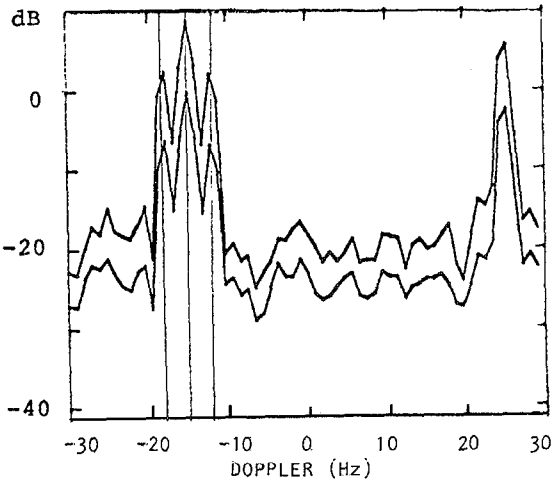

Fig. 5. Conventional beamformer doppler spectrum for simulation experiment.

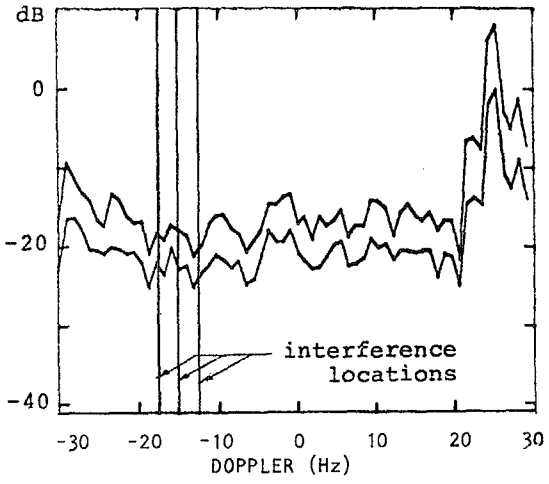

Fig. 6. Fully digital adaptive array doppler spectrum.

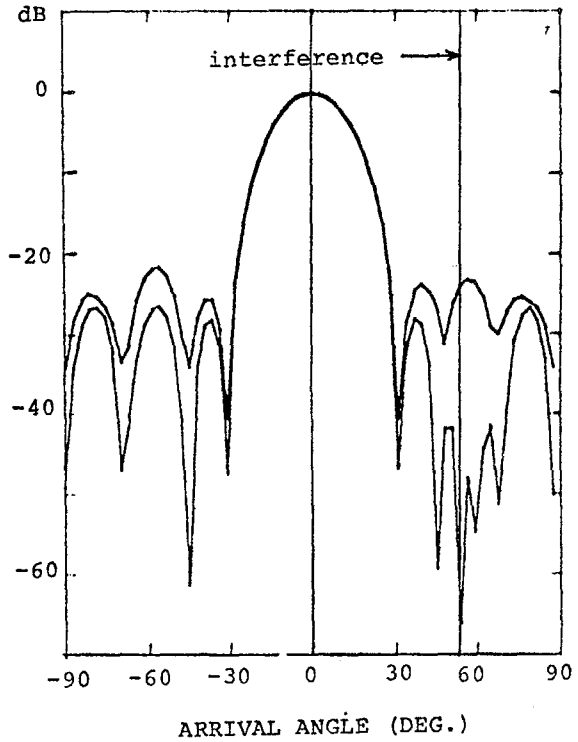

Fig. 7. Fully digital adaptive array beam pattern.

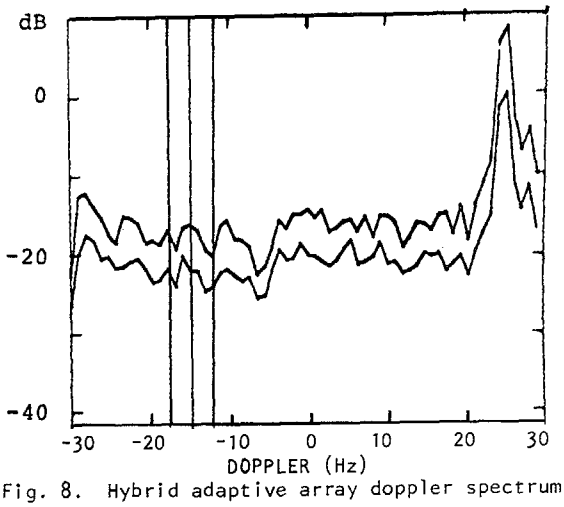

Fig. 8. Hybrid adaptive array doppler spectrum.

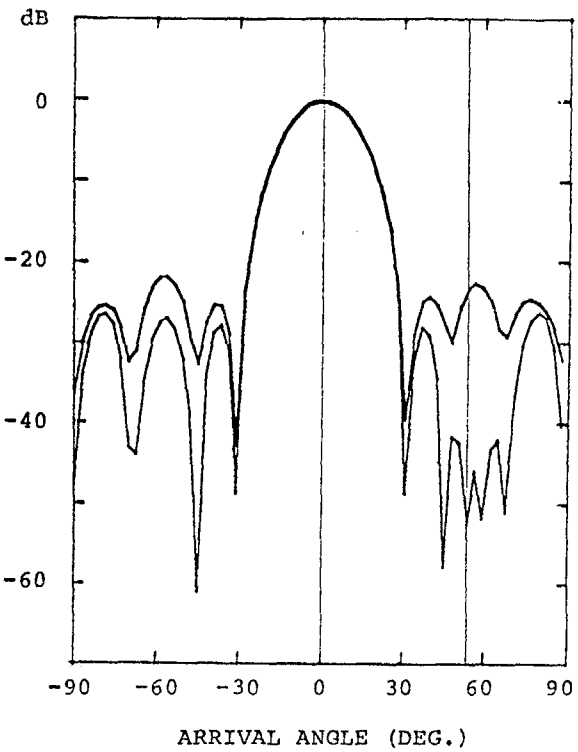

Fig. 9. Hybrid adaptive array beam pattern.